

CHAPTER 6

EXPERIMENTAL WORK

6.1 FABRICATION OF ORGANIC SOLAR CELLS

Various processes involved in the designing and fabrication of solar cells (organic/polymer solar cells in this report) are described in detail.

Substrate cleaning process

1. First, a substrate for the solar cells is used, in this case a transparent electrode made of Indium-Tin-Oxide covered glass. These glass plates are made such that they conduct only on one side.
2. The substrates are cut to the appropriate sizes.
3. A number is scratched onto the glass to mark the non-conductive side.



Fig. 6.1 Patterning of ITO

4. The Indium-Tin-Oxide (ITO) electrodes should be removed from some parts of the glass side to avoid shorts. Etching the ITO in an acidic bath does this.
5. To avoid etching away all the ITO, cover parts of the glass slide with a mask. (According to the size and shape we want) This is done with black adhesive tape, which covers only the parts of the glass, where the ITO coating should stay.
6. To etch the ITO away, the substrates are immersed in 3:1 solution of hydrochloric acid and water i.e. 25% solution of acid in water. To speed up the reaction the beaker is put into ultrasonic bath and zinc powder is added (5mg in 50ml HCl).
7. After the etching process, the substrates are rinsed with deionized water to remove the acid. Under the adhesive tape, the ITO was not etched; it now covers an area of the intended shape and size.
8. The substrates are cleaned for half an hour in special cleaning soap Solution. For better results this is done in a heated Ultrasonic bath.
Note: Because of the extremely small thickness of the active layers in the organic solar cell, a very thorough cleaning is necessary to avoid shorts or bad contacts between the layers.
9. Further cleaning is done. ITO coated substrates are washed in acetone heated at 100° C. This is followed by cleaning in trichloroethane followed by propanol at 100° C for 15 minutes.

10. The spatula is washed with acetone and P3HT and PCBM are weighed on the butter paper (after noting its weight).
11. 20 mg of P3HT (Poly-hexyl-thiophene), a p-type semi conducting polymer and PCBM, soluble derivative of Buckminster fullerene C₆₀ are weighed. They are each transferred into a vial containing 1ml of chlorobenzene, (20mg/ml).
12. The vials are then kept in an ultrasonic bath for half an hour. The frequency set is 35 kHz for making nano-solutions.
13. The substrates are then allowed to dry in an oven at 120⁰ C for 30minutes.
14. ITO coated substrates are subjected to plasma in a plasma thermal evaporator for 5 minutes for the removal of any leftover dirt or particles.
15. ITO covered side of the substrates is now coated with PEDOT: PSS, a transparent conductive polymer that is needed to enhance the contact between the ITO electrode and the active layer. To get a good film quality, the PEDOT: PSS solution has to be filtered.



Fig 6.2 Vacuum oven

16. The optimal film thickness is between 50 and 100 nm. This is achieved by using spin coating technique. In this method the polymer solution is distributed evenly on a glass substrate, which is subsequently rotated at 2000 rpm for 2 minutes. Due to centrifugal forces, a very thin and homogeneous film of the polymer is coated on the surface of the substrate. Then it is cured at 120 °C for 15 mins in a vacuum oven.



Fig 6.3(a) Spin Coater



Fig 6.3(b) Micro pipette and vials

17. The above synthesis Ag colloidal solution was then spin-cast a top the ITO and PEDOT: PSS-coated glass substrate (1000 rpm for 2 mints). The substrates were then dried at 120⁰ C for 15min in vacuum oven.
18. As the active layer of the solar cell is sensitive to atmospheric oxygen and water, the following steps are performed in inert environment glove box.
19. The transfer from and to the glove box is done via an air lock. The lock containing the substrates is evacuated and then filled with nitrogen.
20. The above synthesis active layer (P3HT: PCBM) is also deposited by the spin coating technique. Heating of the substrate to 120°C for 20 mints ensures a fast evaporation of the solvent.
21. When the solvent has evaporated completely, a thin film of P3HT and PCBM with a thickness of about 200nm remains on the surface of the substrate.



Fig. 6.4 Glove Box

22. To finish the solar cells, the metal back electrode has to be evaporated. A mask is aligned to the substrate, so that the metal electrode is deposited only on the area where it is needed.



Fig 6.5 (a) Mask for electrode deposition



Fig 6.5 (b) Equipment for electrode deposition

The evaporation of the metals is done from a small tungsten boat containing the desired metal (aluminum) on which a high current is applied. Thus the boat is heated up and the material evaporates.

23. The process is done in high vacuum, so that the evaporated metal can condense on the substrates as thin films without colliding with gas molecules in between. The film thickness is monitored by a quartz crystal microbalance.

24. The metal electrode is an approx. 100 nm thick layer of aluminum. To optimize the performance of the solar cells, they have to be heated for a few minutes after the final deposition and afterwards cooled down slowly to avoid thermal stress.
25. The finished solar cells degrade quickly when they are in contact with oxygen and water in the atmosphere. Because of that, the solar cells have to be sealed before they can be measured outside the glove box.
26. To seal the solar cells, a cleaned glass plate is glued to the backside of the solar cell with a two-component epoxy resin.
27. Both sets of PV devices (control and experiment) were fabricated during the same batch processing. The active device area (A) was 0.01cm².
28. Now the solar cells are ready. Of course, it is now of high interest to characterize the performance of the solar cells. First, the two contacts of the solar cells are connected to the measurement equipment and the current through the solar cell is measured without illumination. Afterwards the performance of the solar cell under solar irradiation is measured.
29. As the sun is not shining very regularly everywhere, solar cells under natural sunlight illumination are hard to characterize and compare. That is why there are standard lamps giving similar power and solar spectral characteristics.
30. In dark, the solar cell current-voltage (short-I-V) characteristic behaves like a diode. If a negative bias is applied, a small negative current is flowing. At positive applied voltages, the current is much higher. Under illumination, the I-V curve is shifted so in some range the current is negative, even though a positive voltage is applied. In this range, the solar cell generates power.



Fig 6.6 (a) Equipment for electrode deposition

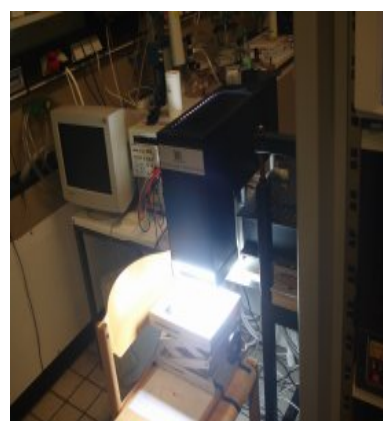


Fig 6.6 (b) Characterization of Cells

31. The $J-V$ curves were measured with a Keithley Source Measuring unit sweeping from -1 V to $+1$ V. The electrodes were ITO and Al. $J-V$ curves give important parameters to describe a solar cell and I_{SC} and V_{OC} are calculated.
32. The maximum of power is generated in the maximum power point. The maximum power output divided by the power of the incoming light is the overall power efficiency of the solar cell.

6.2 SYNTHESIS OF ZnS NANOPARTICLES

ZnS has a wide band gap of 3.5 - 3.8 eV at room temperature and the band gap can be tuned in the UV region. It is an important inorganic material for a variety of applications including photoconductors, solar cells, field effect transistors, sensors, transducers optical coatings and light-emitting materials. It has been investigated extensively, because of its potential optical

applications. ZnS doped with various transition metal ions such as manganese is an efficient light emitting material. Nanostructured materials have been synthesized by many simple methods such as wet chemical method, solid-state reaction method, etc. The purpose of the present work is to synthesize ZnS nanoparticles using aqueous chemical method and investigate the properties such as size, structure, band gap, absorption and luminescence.

The synthesis of ZnS nanoparticles was carried out by aqueous chemical method using zinc chloride and sodium sulfide as source materials. All the reagents were of analytical grade and used without further purification. The entire process was carried out in distilled water for its inherent advantages of being simple and environment friendly. All steps of the synthesis were performed at low temperature and ambient conditions. In a typical preparation, solution of 1 M zinc chloride was prepared in 100 ml of deionized water and then the solution of 1 M sodium sulfide was added drop wise to the solution which was kept on stirring using a magnetic stirrer at 70°C, which resulted in formation of ZnS nano colloid. The nanoparticles were collected by centrifugation at 2000 rpm for 15 minutes. And further purification was made by ultrasonic bath. The resultant product was finally dried at 1200°C for 2 hours.

6.3 APPARATUS USED

During solar cell designing and fabrication, various processes and techniques are performed to assure that the appropriate material with suitable properties is synthesized. Some of the instruments utilized during the fabrication process are given below.

6.3.1 Spin Coating System

Spin coating is a technique by which very thin films are deposited onto a solid substrate. To fabricate thin polymer films, the polymer is first dissolved in a volatile solvent (e.g. chlorobenzene for P3HT:PCBM). If a drop of solution is placed on a substrate, it can flow to form a metastable, continuous film or form a droplet on the surface, depending on the "wettability" of the substrate. By spinning the substrate, the droplet is forced to spread out while the solvent evaporates. If deposition conditions such as choice of solvent, solution concentration and spin speed are chosen correctly, a thin film of uniform thickness is deposited on the substrate.

Spin coating is a procedure used to apply uniform thin films to flat substrates. In short, an excess amount of a solution is placed on the substrate, which is then rotated at high speed in order to spread the fluid by centrifugal force. A machine used for spin coating is called a spin coater, or simply spinner.



Fig 6.7 Spin coating system

Rotation is continued while the fluid spins off the edges of the substrate, until the desired thickness of the film is achieved. The applied solvent is usually volatile, and simultaneously evaporates. So, the higher the angular speed of spinning, the thinner the film. The thickness of the film also depends on the concentration of the solution and the solvent. Spin coating is widely used in micro fabrication, where it can be used to create thin films with thicknesses below 10 nm.

6.3.2 Ultrasonic Bath

An ultrasonic bath is a cleaning device that uses ultrasound (usually from 15–400 kHz). In an ultrasonic bath, the object to be mixed is placed in a chamber containing a suitable ultrasound conducting fluid (an aqueous or organic solvent, depending on the application). An ultrasound generating transducer built into the chamber, or lowered into the fluid, produces ultrasonic waves in the fluid by changing size in concert with an electrical signal oscillating at ultrasonic frequency. This creates compression waves in the liquid of the tank which ‘tear’ the liquid apart, leaving behind many millions of microscopic ‘voids’ or ‘partial vacuum bubbles’ (cavitation). These bubbles collapse with enormous energy; temperatures of 10,000 K and pressures of 50,000 lbs per square inch have been reported. Transducers are usually piezoelectric material (e.g. lead zirconate titanate or barium titanate), and sometimes magnetostrictive (made of a material such as nickel or ferrite).



Fig 6.8 Ultrasonic bath

6.3.3 Glove Box

A glovebox (or glove box) is a sealed container that is designed to allow one to manipulate objects while being in a different atmosphere from the object. Built into the sides of the glovebox are two gloves arranged in such a way that the user can place his or her hands into the gloves and perform tasks inside the box without breaking the seal or allowing potential injury. Part or the entire box is usually transparent to allow the user to see what is being manipulated. Two types of glove boxes exist:

1. Allows a person to work with hazardous substances, such as radioactive materials or infectious disease agents.
2. Allows manipulation of substances that must be contained within a very high purity inert atmosphere, such as argon or nitrogen. It is also possible to use a glove box for manipulation of items in a vacuum chamber.

Inert atmosphere work

The argon in a glove box is pumped through a series of treatment devices which remove solvents, water and oxygen from the gas. Heated copper metal (or some other finely divided metal) is commonly used to remove oxygen; this oxygen removing column is normally regenerated by passing a hydrogen/nitrogen mixture through it while it is heated, the water formed is passed out of the box with the excess hydrogen and nitrogen.



Fig 6.9 Glove box

6.3.4 Thermal Evaporator

Evaporation is a common method of thin film deposition. The source material is evaporated in a vacuum. The vacuum allows vapor particles to travel directly to the target object (substrate), where they condense back to a solid state. Evaporation is used in microfabrication, and to make macro-scale products such as metalized plastic film.

Evaporation involves two basic processes: a hot source material evaporates and condenses on the substrate. It resembles the familiar process by which liquid water appears on the lid of a boiling pot. However, the gaseous environment and heat source are different.

Evaporation takes place in a vacuum, i.e. vapors other than the source material are almost entirely removed before the process begins. In high vacuum (with a long mean free path), evaporated particles can travel directly to the deposition target without colliding with the background gas. At a typical pressure of 10^{-4} Pa, an 0.4-nm particle has a mean free path of 60 m. Hot objects in the evaporation chamber, such as heating filaments, produce unwanted vapors that limit the quality of the vacuum.

Evaporated atoms that collide with foreign particles may react with them; for instance, if aluminium is deposited in the presence of oxygen, it will form aluminium oxide. They also reduce the amount of vapor that reaches the substrate, which makes the thickness difficult to control.

Evaporated materials deposit non uniformly if the substrate has a rough surface. Because the evaporated material attacks the substrate mostly from a single direction, protruding features block the evaporated material from some areas. When evaporation is performed in poor vacuum or close to atmospheric pressure, the resulting deposition is generally non-uniform and tends not to be a continuous or smooth film. Rather, the deposition will appear fuzzy.

Any evaporation system includes a vacuum pump. It also includes an energy source that evaporates the material to be deposited. Many different energy sources exist. In the thermal method, the source material is placed in a crucible, which is radiatively heated by an electric

filament. Alternatively, the source material may be hung from the filament itself (filament evaporation).

Optimization

- Purity of the deposited film depends on the quality of the vacuum, and on the purity of the source material.
- The thickness of the film will vary due to the geometry of the evaporation chamber. Collisions with residual gases aggravate nonuniformity of thickness.
- In order to deposit a material, the evaporation system must be able to melt it. This makes refractory materials such as tungsten hard to deposit by methods that do not use electron-beam heating.



Fig 6.10 Thermal Evaporator

6.3.5 Balance

An analytical balance is used to measure the mass to a very high degree of precision and accuracy. The measuring pans of a high precision (0.1 mg or better) analytical balance are inside a transparent enclosure with doors so that dust does not collect or any air turbulence in the room does not affect the balance's operation. The use of a vented balance safety enclosure, which has uniquely designed acrylic airfoils, allows a smooth turbulence-free airflow that prevents balance from fluctuation and the measure of the mass down to $1\mu\text{g}$ can be performed without loss of the product. Also, the sample must be at room temperature to prevent natural convection from forming air currents inside the enclosure, affecting the measure of mass.



Fig 6.11 Balance

6.4 DEVICE CHARACTERIZATION

Characterization of ZnS nanoparticles is done with the help of various techniques such as UV-Visible spectroscopy, Atomic Force Microscopy (AFM), X-ray Diffractometer (XRD), Scanning Electron Microscopy (SEM), Transmission Electron Microscopy (TEM) and Photoluminescence (PL). These are studied and discussed below.

6.4.1 UV-Visible Spectroscopy

The room temperature UV-Vis spectrum of the clear solution of ZnS nanoparticle in distilled water obtained from the synthesis is shown in Figure 6.12 using Perkin Elmer Spectrophotometer in the absorption mode. It exhibits the absorption edge of ZnS nanoparticles at 317 nm (3.8 eV), which is slightly blue shifted from that of bulk ZnS (340 nm, $E_g = 3.65$ eV). This closeness of the absorption peak to the bulk ZnS crystals are attributed to the near-band-edge free excitons. The broadening of the absorption spectrum could be due to the quantum confinement of the nanoparticles.

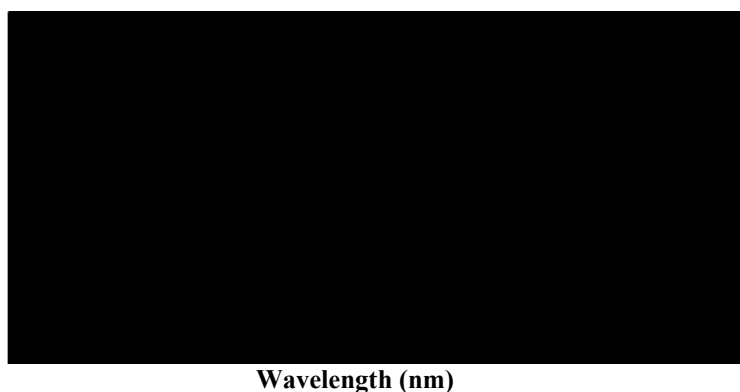


Fig 6.12 UV-vis absorption spectra (baseline corrected with a background of distilled water)

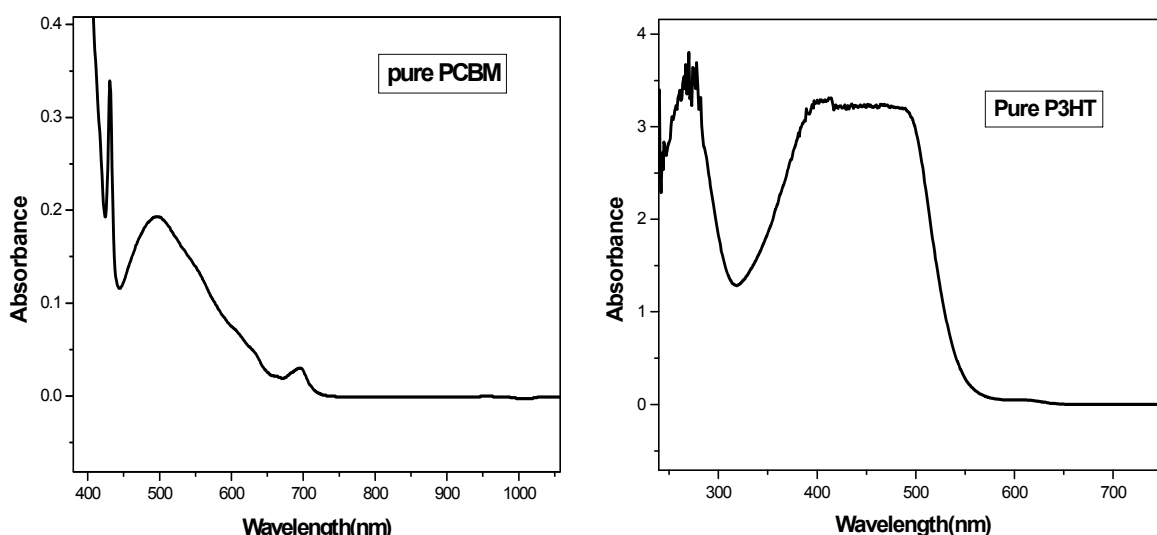


Fig 6.13 UV-vis absorption spectra of the (a) PCBM solution (b) P3HT solution showing peak (the absorption baseline corrected with a background of chlorobenzene).

Absorption spectra of the PCBM solution are taken showing a peak at 490 nm and the same is shown in figure 6.13 (a). Figure 6.13 (b) Shows UV-vis absorption spectra of the P3HT solution showing a broad wavelength range of 420-530 nm (the transmission is baseline

corrected with a background of chlorobenzene). Both P3HT and PCBM solutions are mixed in 1:1 ratio with concentration of 20mg/ml and absorbtion peak is taken. Then ZnS nanoparticles are added and UV-Via absorbtion is taken.

6.4.2 Atomic Force Microscopy

Atomic force microscope (AFM) measurements were done in tapping mode. AFM pictures were applied to check the roughness of the films: this was used to see the distribution of the materials in bulk heterojunction cells, to estimate the size of the zinc sulfide nano-particles and to see if the material makes a real film or if there are just islands of the material within the device.

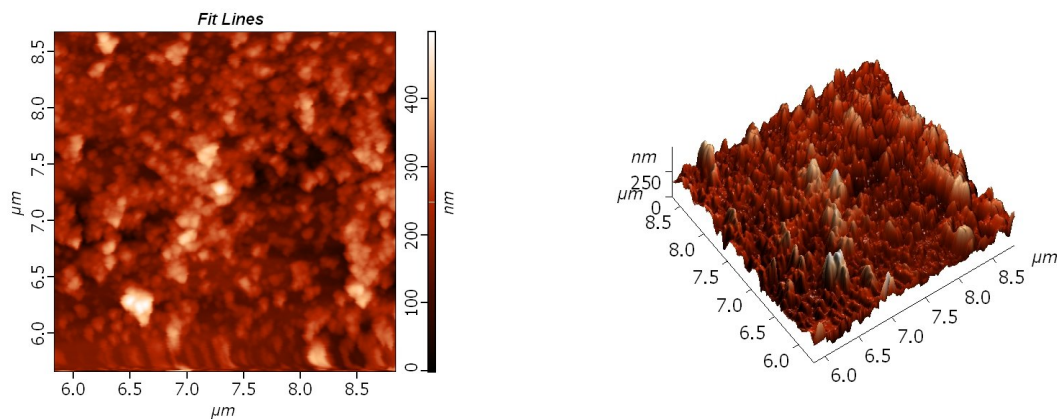


Fig 6.14 (a) AFM picture of a spin coated ZnS nanoparticles film on ITO/PEDOT: PSS on glass and (b) 3-D AFM picture of a spin coated ZnS nanoparticles film on ITO glass

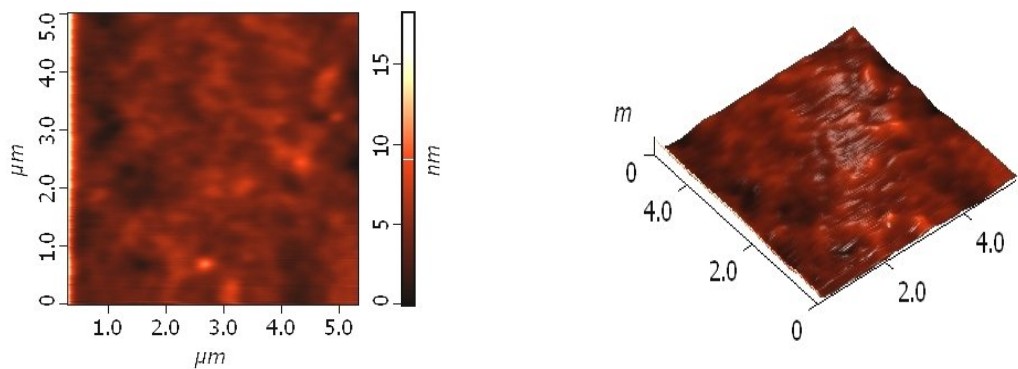


Fig 6.15(a) AFM image of PEDOT-PSS spin-coated on cleaned ITO and (b) 3-D AFM image of PEDOT-PSS spin-coated on cleaned ITO

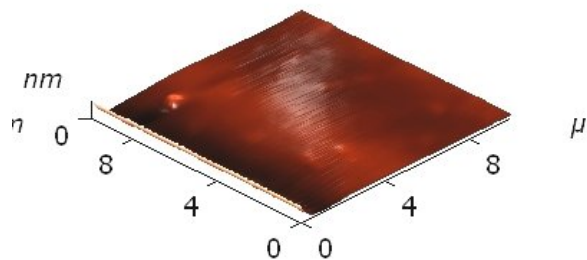


Fig 6.16 AFM-picture of a PCBM:P3HT bulk heterojunction solar cell on ITO glass

It shows a very high roughness of the layer. It can be assumed that the nanoparticles aggregated to very big clusters and that the layer is highly phase separate. From AFM image, morphology of the nanoparticles can be observed, which in this case is spherical.

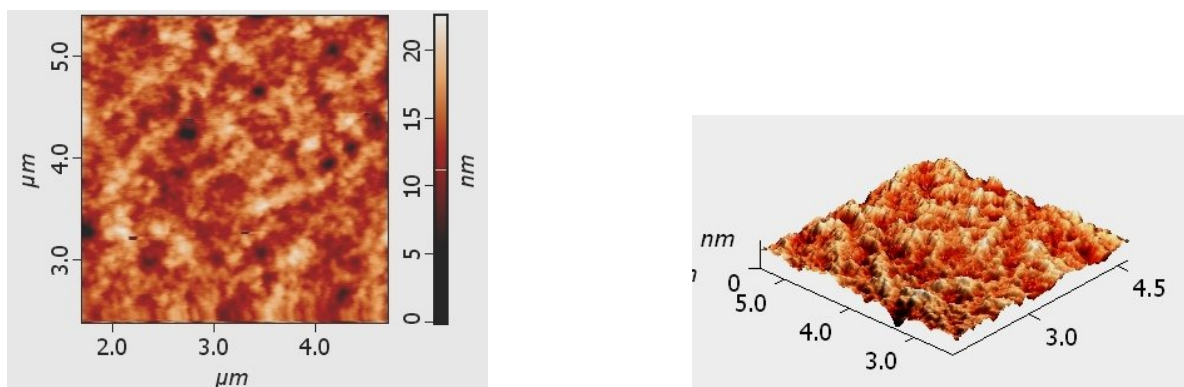


Fig 6.17 AFM-picture of ZnS NPs on PCBM: P3HT bulk heterojunction solar cell on ITO glass

6.4.3 X-ray Diffractometer

The crystallographic structure of the particles was determined by powder X-ray diffraction. XRD of the film is taken. Film is made by spin coating and drying them in the vacuum oven. Figure shows the X-ray diffraction pattern of films of:

- A. PEDOT: PSS layer on glass of size 1x1cm
- B. PEDOT: PSS/ZnS nanoparticles layer on glass

As one can see the location of the pattern is in not much good agreement with the Joint Committee on Powder Diffraction Standards (JCPDS), this is because it was multilayer film and there was too much roughness on the film.

Figure 6.18 shows X-ray diffraction pattern of PEDOT: PSS layer on glass. Instead the PEDOT: PSS is a crystalline material there is no intense peak in this film because there was very much roughness.

Figure 6.19 shows X-ray diffraction pattern of ZnS nanoparticles spin-coated on PEDOT: PSS layer. In this film there is prominent peak at $2\theta = 28.028^\circ$ oriented along the (111) direction and other prominent peaks observed at 47.597° (220) and 56.674° (311) indicate that ZnS might be present in the multilayer film.

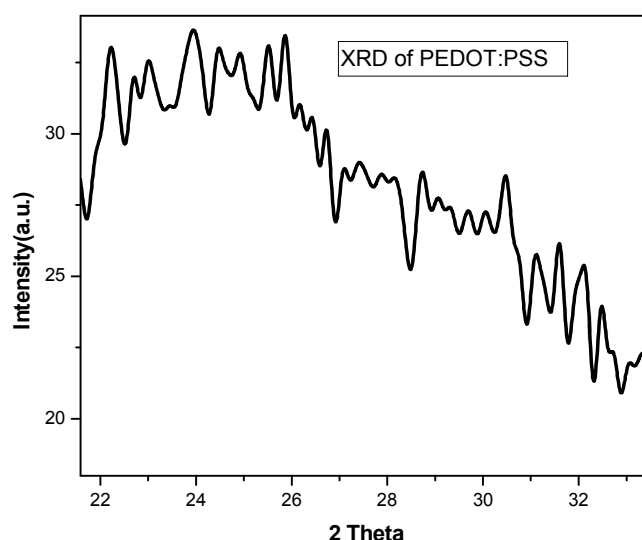


Fig 6.18 X-ray diffraction pattern of PEDOT: PSS layer on glass

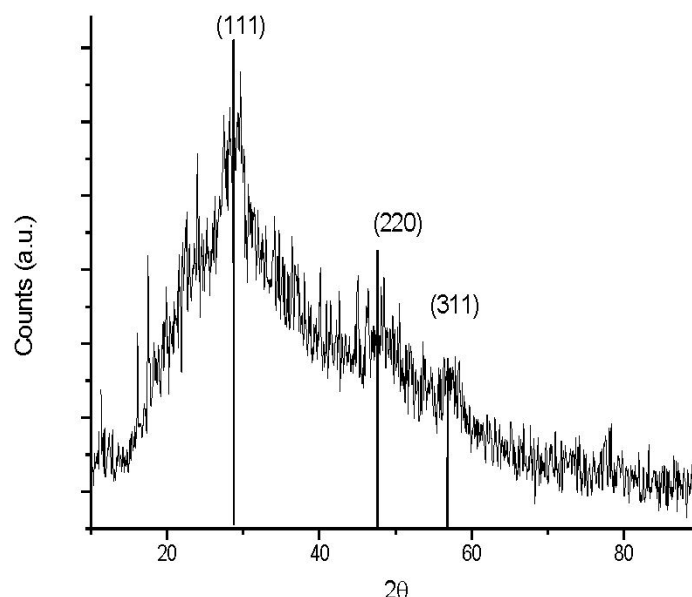


Fig 6.19 X-ray diffraction pattern of ZnS nanoparticles spin-coated on PEDOT: PSS layer

The XRD study indicates the presence of zinc sulfide (ZnS) nano particles, but some peaks slightly shifted due to the multilayer. Wide peaks in the X-rays diffraction pattern suggests presence of nanometric particles, since the chosen reaction was designed to produce ZnS, then elucidated peaks in the diffraction pattern should be from ZnS. Table 6.1 shows experimentally obtained X-ray diffraction angle and the standard diffraction angle of Ag specimen.

Table 6.1 Experimental and standard diffraction angles of ZnS specimen

Experimental diffraction angle [2θ in degrees]	Standard diffraction angle [2θ in degrees]
45	44.3
79.12	77.5

From this study, considering the peak at 45 degrees, average particle size has been estimated by using Debye-Scherrer formula

$$D = \frac{0.9\lambda}{W \cos \theta}$$

Where ' λ ' is wavelength of X-Ray (0.1541 nm), ' θ ' is the diffraction angle and 'D' is particle diameter (size), 'W' is the FWHM of diffraction peak. The average particle size can then be calculated. The average particle size from the most intense peak was estimated to be 12 nm.

6.4.4 Scanning Electron Microscopy (SEM)

Figure 6.20 shows the SEM image of ZnS nanoparticles. The morphology of the ZnS resembles the bean-like nanostructure. The particles are spherical and agglomerated to form larger particles. To verify the morphological scheme obtained from XRD, the data from the transmission electron microscopy (TEM) was studied.

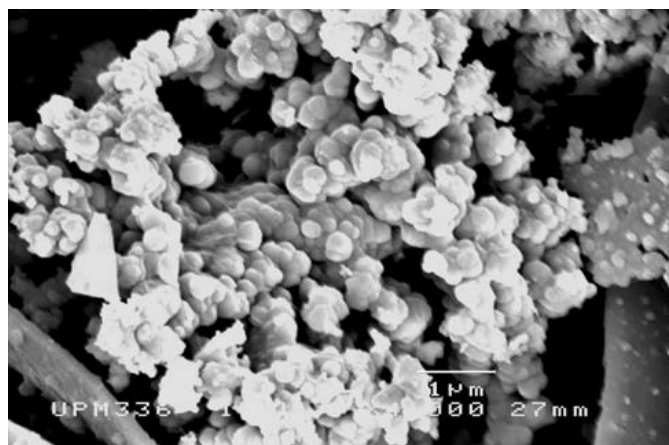


Fig 6.20 SEM image of ZnS nanoparticles

6.4.5 Photoluminescence (PL)

To investigate the luminescence properties, the PL spectra of the as-synthesized ZnS nanoparticles were performed. Figure 6.21 shows the emission spectra and we can see the strong emission bands at about 388 nm and 398 nm. Usually for semiconductor nanocrystals, two emission peaks can be observed- the exciton and the trapped luminescence. The exciton emission peak is sharp and the trapped emission is broad. The emission bands showed in the spectra can be attributed to band gap emission and the strong band gap emission demonstrates the high crystalline nature of the as-synthesized particles. The emission peak around (~3.14 eV) could be attributed to the recombination of electrons from the energy level of sulphur vacancies with the holes from the valence band. Photoluminescence (PL) investigations revealed the presence of two broad emission bands. The ZnS thickness significantly influenced the PL intensities. Such ZnS nanoparticles could be used to design advanced semiconductor nano devices such as optoelectronics and gas sensors.

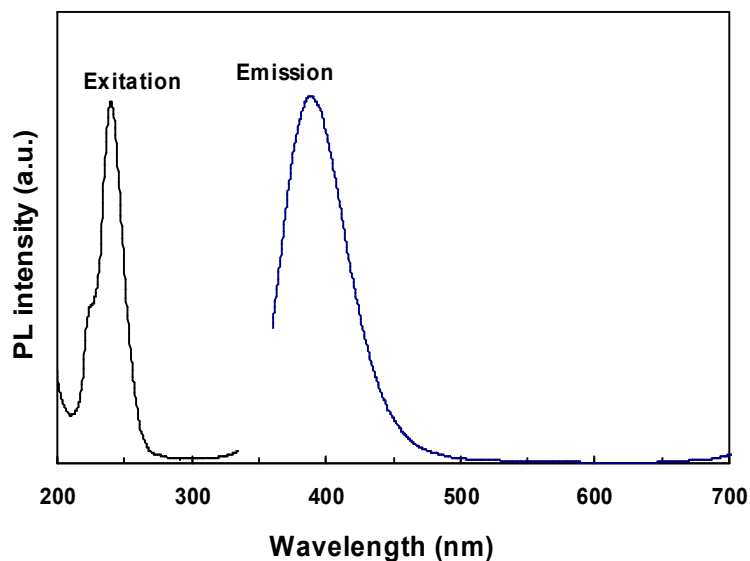


Fig 6.21 Photoluminescence spectra for obtained dispersions

6.4.6 Transmission Electron Microscopy (TEM)

Figure 6.22(a) represents a typical Transmission Electron Microscopy (TEM) image. This image shows the ring pattern and confirms the peak positions than in the X-rays diffraction pattern are far less defined than those produced by bulk materials. The particles are seen to be nearly spherical and the sample morphology mainly consisted of tightly agglomerated particles. The ZnS nanocrystals are significantly smaller in size with a mean diameter of 6.8 nm with a standard deviation of 1.4 nm. Figure 6.22 (b) shows the agglomeration of ZnS particles under TEM observation. The tendency to form nanoclusters due to the high surface energy of nanoparticles is an unavoidable phenomenon as observed in the present case.

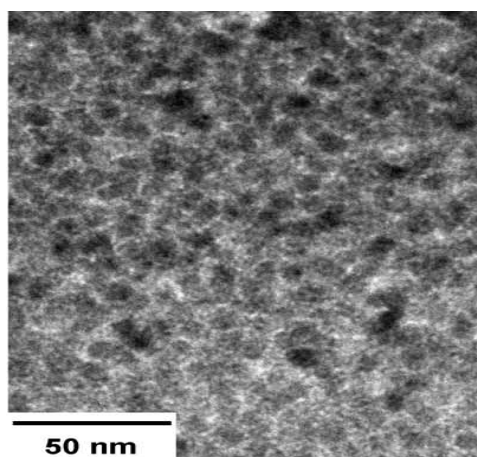
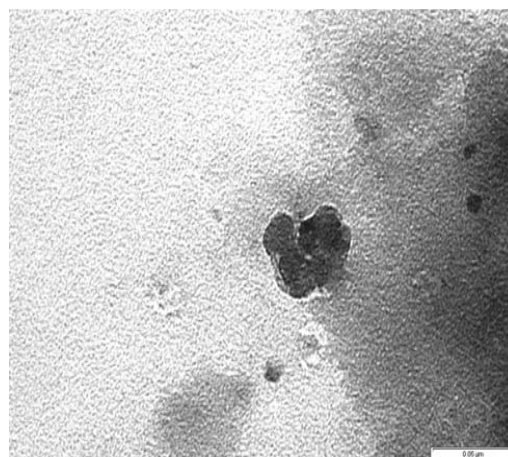


Fig 6.22 (a) TEM image of ZnS nanocrystals



(b) Agglomeration of ZnS NPs as observed under TEM image

6.4.7 Fourier Transform Infrared Spectroscopy (FTIR)

The FTIR spectrum for ZnS nanoparticles is presented in Figure 6.23. The spectrum in the range 300-4000 cm^{-1} was showing IR absorption due to the various vibrations involved.

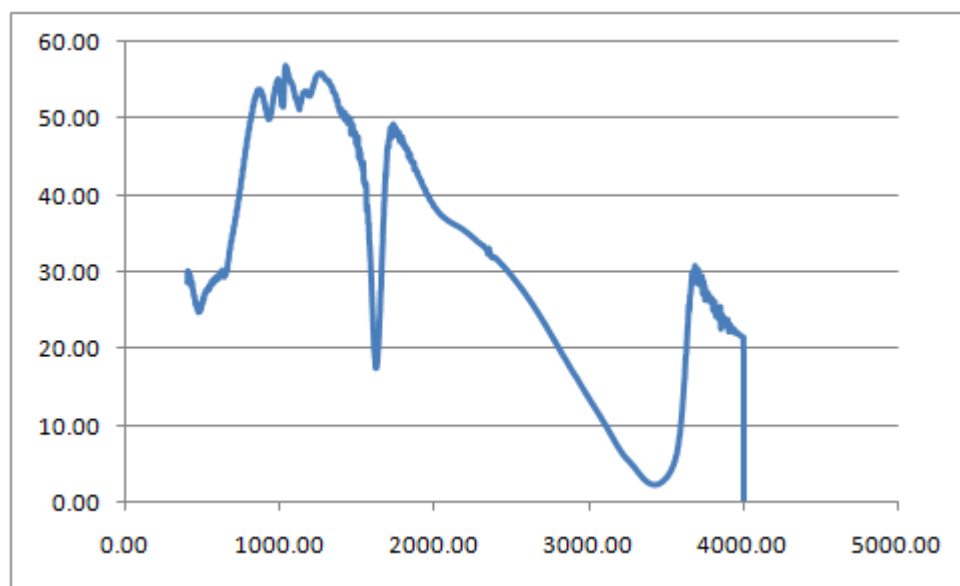


Fig 6.23 FTIR spectrum of ZnS nanoparticles

1/cm

6.5 RESULTS AND DISCUSSION

I-V data taken by Keithley Source measuring unit

The experiment is started with reference device (ITO/PEDOT: PSS/P3HT: PCBM in chlorobenzene/Al) and control device (ITO/PEDOT:PSS/ZnS nanoparticles in chlorobenzene/Al). Figure 6.24 shows J-V characteristics of reference device (ITO/PEDOT:PSS/ P3HT:PCBM/Al) and control device (ITO/PEDOT:PSS/ZnS/Al) before annealing under darkness.

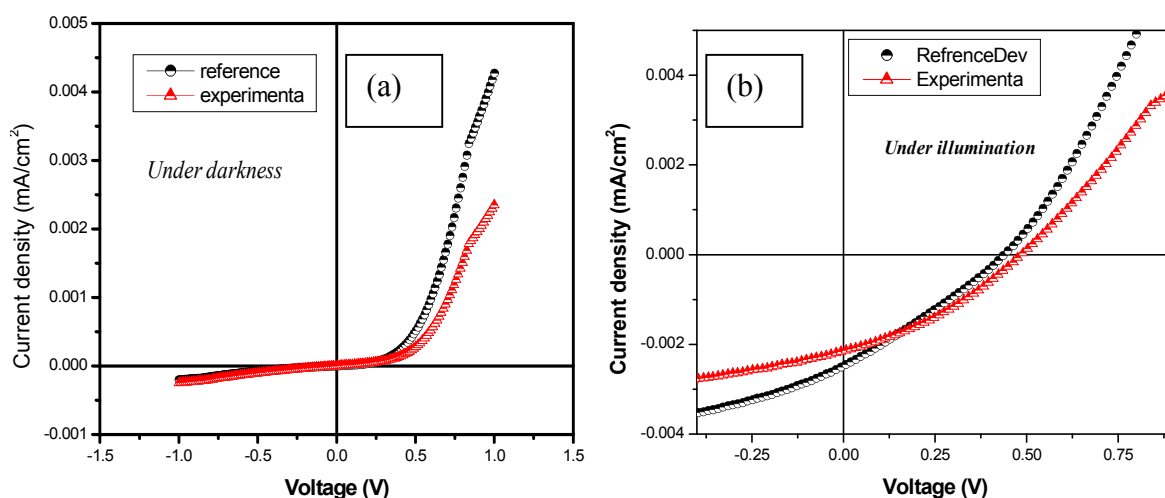


Fig 6.24 J-V characteristics of the reference device (ITO/PEDOT:PSS/P3HT: PCBM/Al) and control device (ITO/PEDOT:PSS/ZnS/Al) (a) in darkness and (b) in light.

The sample data obtained from the characterization of the one of the Organic Solar Cells i.e. the current and voltage data from the cell in dark and under illumination is as follows:

Cell Characteristics in Light

VOLTAGE	CURRENT	CURRENT DENSITY	POWER
(V)	(I)	(J)	(P)
#####	-8.05E-04	-9.94E-03	9.94E-03
-9.87E-01	-8.27E-04	-1.03E-02	1.02E-02
-9.73E-01	-7.85E-04	-9.81E-03	9.55E-03
-9.60E-01	-7.47E-04	-9.34E-03	8.96E-03
-9.46E-01	-7.33E-04	-9.16E-03	8.67E-03
-9.33E-01	-8.10E-04	-1.01E-02	9.44E-03
-9.19E-01	-7.55E-04	-9.43E-03	8.68E-03
-9.06E-01	-7.42E-04	-9.28E-03	8.41E-03
-8.93E-01	-7.97E-04	-9.96E-03	8.89E-03
-8.79E-01	-7.62E-04	-9.53E-03	8.38E-03
-8.66E-01	-7.43E-04	-9.29E-03	8.05E-03
-8.52E-01	-7.71E-04	-9.64E-03	8.21E-03
-8.39E-01	-7.66E-04	-9.57E-03	8.03E-03
-8.26E-01	-7.48E-04	-9.35E-03	7.72E-03
-8.12E-01	-7.23E-04	-9.04E-03	7.34E-03
-7.99E-01	-7.71E-04	-9.64E-03	7.70E-03
-7.85E-01	-7.76E-04	-9.70E-03	7.62E-03
-7.72E-01	-7.18E-04	-8.98E-03	6.93E-03
-7.58E-01	-7.58E-04	-9.47E-03	7.18E-03
-7.45E-01	-7.38E-04	-9.22E-03	6.87E-03
-7.32E-01	-7.41E-04	-9.26E-03	6.78E-03
-7.18E-01	-6.88E-04	-8.60E-03	6.18E-03
-7.05E-01	-6.95E-04	-8.69E-03	6.12E-03
-6.91E-01	-7.43E-04	-9.29E-03	6.42E-03
-6.78E-01	-7.23E-04	-9.03E-03	6.12E-03
-6.65E-01	-7.44E-04	-9.30E-03	6.18E-03
-6.51E-01	-6.94E-04	-8.68E-03	5.65E-03
-6.38E-01	-7.25E-04	-9.06E-03	5.78E-03
-6.24E-01	-6.85E-04	-8.56E-03	5.34E-03
-6.11E-01	-7.26E-04	-9.07E-03	5.54E-03
-5.97E-01	-6.74E-04	-8.43E-03	5.04E-03
-5.84E-01	-6.79E-04	-8.48E-03	4.95E-03
-5.70E-01	-7.17E-04	-8.96E-03	5.11E-03
-5.57E-01	-6.97E-04	-8.71E-03	4.85E-03
-5.44E-01	-7.20E-04	-9.00E-03	4.89E-03
-5.30E-01	-6.68E-04	-8.36E-03	4.43E-03
-5.17E-01	-7.00E-04	-8.75E-03	4.52E-03
-5.03E-01	-7.16E-04	-8.95E-03	4.51E-03
-4.90E-01	-6.73E-04	-8.41E-03	4.12E-03
-4.76E-01	-6.50E-04	-8.12E-03	3.87E-03
-4.63E-01	-6.92E-04	-8.64E-03	4.00E-03
-4.50E-01	-6.76E-04	-8.46E-03	3.80E-03
-4.36E-01	-6.27E-04	-7.84E-03	3.42E-03
-4.23E-01	-6.40E-04	-7.99E-03	3.38E-03
-4.09E-01	-6.80E-04	-8.50E-03	3.48E-03
-3.96E-01	-6.29E-04	-7.86E-03	3.11E-03
-3.82E-01	-6.11E-04	-7.64E-03	2.92E-03
-3.69E-01	-6.80E-04	-8.50E-03	3.14E-03
-3.56E-01	-6.28E-04	-7.86E-03	2.79E-03

-3.42E-01	-6.11E-04	-7.64E-03	2.62E-03
-3.29E-01	-6.70E-04	-8.38E-03	2.76E-03
-3.15E-01	-6.32E-04	-7.90E-03	2.49E-03
-3.02E-01	-6.14E-04	-7.67E-03	2.32E-03
-2.89E-01	-6.40E-04	-8.00E-03	2.31E-03
-2.75E-01	-6.36E-04	-7.96E-03	2.19E-03
-2.62E-01	-6.17E-04	-7.71E-03	2.02E-03
-2.48E-01	-5.84E-04	-7.30E-03	1.81E-03
-2.35E-01	-6.36E-04	-7.95E-03	1.87E-03
-2.22E-01	-6.17E-04	-7.71E-03	1.71E-03
-2.08E-01	-5.71E-04	-7.13E-03	1.48E-03
-1.95E-01	-6.29E-04	-7.87E-03	1.53E-03
-1.81E-01	-6.12E-04	-7.65E-03	1.39E-03
-1.68E-01	-5.64E-04	-7.05E-03	1.18E-03
-1.54E-01	-6.06E-04	-7.58E-03	1.17E-03
-1.41E-01	-6.04E-04	-7.55E-03	1.06E-03
-1.28E-01	-5.63E-04	-7.03E-03	8.97E-04
-1.14E-01	-5.65E-04	-7.06E-03	8.05E-04
-1.00E-01	-5.30E-04	-6.63E-03	6.66E-04
-8.73E-02	-5.81E-04	-7.26E-03	6.33E-04
-7.39E-02	-5.33E-04	-6.66E-03	4.92E-04
-6.03E-02	-5.36E-04	-6.70E-03	4.04E-04
-4.69E-02	-5.55E-04	-6.94E-03	3.26E-04
-3.35E-02	-5.43E-04	-6.79E-03	2.28E-04
-2.02E-02	-5.52E-04	-6.91E-03	1.39E-04
-6.64E-03	-5.07E-04	-6.34E-03	4.21E-05
6.62E-03	5.46E-04	-6.83E-03	-4.52E-05
2.03E-02	-5.08E-04	-6.35E-03	-1.29E-04
3.35E-02	-5.22E-04	-6.52E-03	-2.18E-04
4.70E-02	-4.84E-04	-6.05E-03	-2.84E-04
6.04E-02	-4.81E-04	-6.01E-03	-3.63E-04
7.39E-02	-4.98E-04	-6.23E-03	-4.60E-04
8.71E-02	-4.85E-04	-6.06E-03	-5.28E-04
1.01E-01	-4.82E-04	-6.02E-03	-6.06E-04
1.14E-01	-4.44E-04	-5.55E-03	-6.33E-04
1.27E-01	-4.77E-04	-5.96E-03	-7.60E-04
1.41E-01	-4.58E-04	-5.73E-03	-8.07E-04
1.54E-01	-4.43E-04	-5.54E-03	-8.54E-04
1.68E-01	-4.07E-04	-5.09E-03	-8.54E-04
1.81E-01	-4.05E-04	-5.06E-03	-9.17E-04
1.95E-01	-4.25E-04	-5.31E-03	-1.03E-03
2.08E-01	-4.02E-04	-5.03E-03	-1.05E-03
2.21E-01	-3.97E-04	-4.96E-03	-1.10E-03
2.35E-01	-3.61E-04	-4.51E-03	-1.06E-03
2.48E-01	-3.79E-04	-4.74E-03	-1.18E-03
2.62E-01	-3.61E-04	-4.51E-03	-1.18E-03
2.75E-01	-3.41E-04	-4.26E-03	-1.17E-03
2.89E-01	-3.05E-04	-3.82E-03	-1.10E-03
3.02E-01	-2.93E-04	-3.67E-03	-1.11E-03
3.15E-01	-3.00E-04	-3.75E-03	-1.18E-03
3.29E-01	-2.72E-04	-3.40E-03	-1.12E-03
3.42E-01	-2.56E-04	-3.20E-03	-1.09E-03
3.56E-01	-2.20E-04	-2.75E-03	-9.79E-04
3.69E-01	-2.20E-04	-2.75E-03	-1.01E-03
3.82E-01	-1.91E-04	-2.39E-03	-9.15E-04
3.96E-01	-1.63E-04	-2.04E-03	-8.06E-04
4.09E-01	-1.27E-04	-1.58E-03	-6.48E-04
4.23E-01	-1.03E-04	-1.28E-03	-5.42E-04

4.37E-01	-7.29E-05	-9.11E-04	-3.98E-04
4.50E-01	-4.94E-05	-6.18E-04	-2.78E-04
4.63E-01	-2.09E-05	-2.61E-04	-1.21E-04
4.76E-01	1.74E-05	2.17E-04	1.04E-04
4.90E-01	5.27E-05	6.58E-04	3.23E-04
5.03E-01	8.48E-05	1.06E-03	5.34E-04
5.17E-01	1.23E-04	1.54E-03	7.98E-04
5.30E-01	1.63E-04	2.04E-03	1.08E-03
5.44E-01	2.03E-04	2.53E-03	1.38E-03
5.57E-01	2.44E-04	3.05E-03	1.70E-03
5.70E-01	2.90E-04	3.63E-03	2.07E-03
5.84E-01	3.32E-04	4.15E-03	2.42E-03
5.97E-01	3.75E-04	4.69E-03	2.80E-03
6.11E-01	4.20E-04	5.25E-03	3.21E-03
6.24E-01	4.71E-04	5.89E-03	3.68E-03
6.38E-01	5.16E-04	6.45E-03	4.12E-03
6.51E-01	5.55E-04	6.93E-03	4.51E-03
6.64E-01	6.17E-04	7.71E-03	5.12E-03
6.78E-01	6.65E-04	8.32E-03	5.64E-03
6.91E-01	7.02E-04	8.78E-03	6.07E-03
7.05E-01	7.56E-04	9.45E-03	6.66E-03
7.18E-01	8.14E-04	1.02E-02	7.31E-03
7.32E-01	8.57E-04	1.07E-02	7.84E-03
7.45E-01	8.94E-04	1.12E-02	8.32E-03
7.59E-01	9.56E-04	1.19E-02	9.06E-03
7.72E-01	1.02E-03	1.27E-02	9.82E-03
7.85E-01	1.06E-03	1.32E-02	1.04E-02
7.99E-01	1.12E-03	1.40E-02	1.12E-02
8.12E-01	1.18E-03	1.47E-02	1.19E-02
8.26E-01	1.23E-03	1.54E-02	1.27E-02
8.39E-01	1.27E-03	1.58E-02	1.33E-02
8.52E-01	1.35E-03	1.69E-02	1.44E-02
8.66E-01	1.41E-03	1.76E-02	1.52E-02
8.79E-01	1.45E-03	1.81E-02	1.59E-02
8.93E-01	1.53E-03	1.91E-02	1.70E-02
9.06E-01	1.59E-03	1.99E-02	1.80E-02
9.20E-01	1.63E-03	2.04E-02	1.87E-02
9.33E-01	1.69E-03	2.11E-02	1.97E-02
9.46E-01	1.64E-03	2.05E-02	1.94E-02
9.60E-01	1.70E-03	2.13E-02	2.04E-02
9.73E-01	1.77E-03	2.21E-02	2.15E-02
9.87E-01	1.86E-03	2.33E-02	2.30E-02
1.00E+00	1.96E-03	2.46E-02	2.46E-02

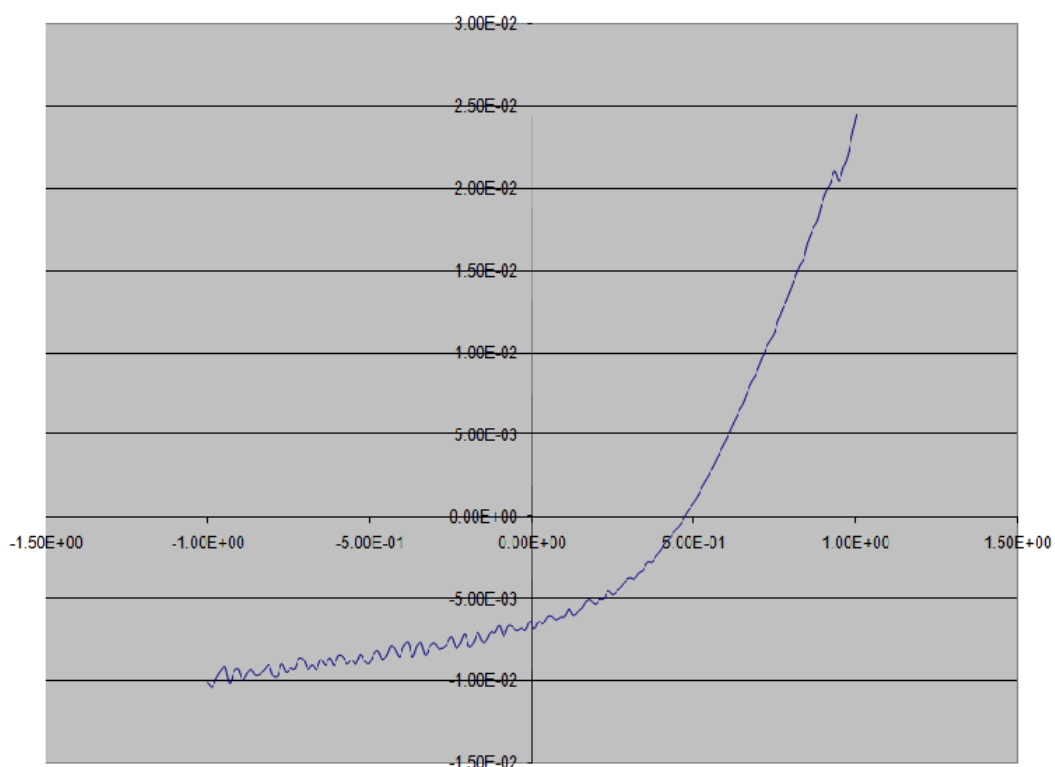


Fig 6.25 Cell characteristics in light

Cell Characteristics in Dark

VOLTAGE (V)	CURRENT (I)	CURRENT DENSITY (J)	POWER (P)
#####	-9.66E-05	-1.21E-03	1.21E-03
-9.87E-01	-9.35E-05	-1.17E-03	1.15E-03
-9.73E-01	-9.03E-05	-1.13E-03	1.10E-03
-9.60E-01	-8.72E-05	-1.09E-03	1.05E-03
-9.46E-01	-8.45E-05	-1.06E-03	1.00E-03
-9.33E-01	-8.19E-05	-1.02E-03	9.55E-04
-9.19E-01	-7.94E-05	-9.92E-04	9.12E-04
-9.06E-01	-7.70E-05	-9.63E-04	8.72E-04
-8.93E-01	-7.44E-05	-9.30E-04	8.30E-04
-8.79E-01	-7.22E-05	-9.02E-04	7.93E-04
-8.66E-01	-7.01E-05	-8.76E-04	7.59E-04
-8.52E-01	-6.81E-05	-8.52E-04	7.26E-04
-8.39E-01	-6.60E-05	-8.25E-04	6.92E-04
-8.25E-01	-6.42E-05	-8.03E-04	6.63E-04
-8.12E-01	-6.22E-05	-7.78E-04	6.32E-04
-7.99E-01	-6.04E-05	-7.55E-04	6.03E-04
-7.85E-01	-5.86E-05	-7.32E-04	5.75E-04
-7.72E-01	-5.69E-05	-7.12E-04	5.49E-04
-7.58E-01	-5.50E-05	-6.87E-04	5.21E-04
-7.45E-01	-5.34E-05	-6.67E-04	4.97E-04
-7.32E-01	-5.18E-05	-6.48E-04	4.74E-04
-7.18E-01	-5.04E-05	-6.30E-04	4.53E-04
-7.05E-01	-4.88E-05	-6.10E-04	4.30E-04
-6.91E-01	-4.72E-05	-5.91E-04	4.08E-04
-6.78E-01	-4.57E-05	-5.72E-04	3.88E-04
-6.64E-01	-4.43E-05	-5.53E-04	3.68E-04
-6.51E-01	-4.29E-05	-5.36E-04	3.49E-04

-6.38E-01	-4.15E-05	-5.18E-04	3.31E-04
-6.24E-01	-4.00E-05	-5.00E-04	3.12E-04
-6.11E-01	-3.87E-05	-4.83E-04	2.95E-04
-5.97E-01	-3.74E-05	-4.68E-04	2.80E-04
-5.84E-01	-3.62E-05	-4.52E-04	2.64E-04
-5.70E-01	-3.51E-05	-4.39E-04	2.50E-04
-5.57E-01	-3.38E-05	-4.23E-04	2.35E-04
-5.44E-01	-3.26E-05	-4.08E-04	2.22E-04
-5.30E-01	-3.15E-05	-3.94E-04	2.09E-04
-5.17E-01	-3.03E-05	-3.79E-04	1.96E-04
-5.03E-01	-2.93E-05	-3.66E-04	1.84E-04
-4.90E-01	-2.81E-05	-3.51E-04	1.72E-04
-4.76E-01	-2.70E-05	-3.38E-04	1.61E-04
-4.63E-01	-2.59E-05	-3.24E-04	1.50E-04
-4.50E-01	-2.49E-05	-3.12E-04	1.40E-04
-4.36E-01	-2.38E-05	-2.98E-04	1.30E-04
-4.23E-01	-2.29E-05	-2.86E-04	1.21E-04
-4.09E-01	-2.19E-05	-2.74E-04	1.12E-04
-3.96E-01	-2.10E-05	-2.63E-04	1.04E-04
-3.83E-01	-2.01E-05	-2.51E-04	9.59E-05
-3.69E-01	-1.91E-05	-2.39E-04	8.82E-05
-3.56E-01	-1.82E-05	-2.28E-04	8.11E-05
-3.42E-01	-1.75E-05	-2.18E-04	7.47E-05
-3.29E-01	-1.66E-05	-2.07E-04	6.81E-05
-3.15E-01	-1.57E-05	-1.96E-04	6.20E-05
-3.02E-01	-1.49E-05	-1.86E-04	5.62E-05
-2.89E-01	-1.41E-05	-1.76E-04	5.07E-05
-2.75E-01	-1.33E-05	-1.66E-04	4.56E-05
-2.62E-01	-1.25E-05	-1.56E-04	4.08E-05
-2.48E-01	-1.17E-05	-1.46E-04	3.63E-05
-2.35E-01	-1.10E-05	-1.37E-04	3.22E-05
-2.21E-01	-1.02E-05	-1.28E-04	2.84E-05
-2.08E-01	-9.56E-06	-1.20E-04	2.49E-05
-1.95E-01	-8.79E-06	-1.10E-04	2.14E-05
-1.81E-01	-8.13E-06	-1.02E-04	1.84E-05
-1.68E-01	-7.48E-06	-9.35E-05	1.57E-05
-1.54E-01	-6.83E-06	-8.53E-05	1.32E-05
-1.41E-01	-6.14E-06	-7.67E-05	1.08E-05
-1.27E-01	-5.54E-06	-6.92E-05	8.82E-06
-1.14E-01	-4.91E-06	-6.13E-05	6.99E-06
-1.01E-01	-4.29E-06	-5.36E-05	5.39E-06
-8.72E-02	-3.69E-06	-4.61E-05	4.02E-06
-7.38E-02	-3.11E-06	-3.89E-05	2.87E-06
-6.03E-02	-2.54E-06	-3.18E-05	1.92E-06
-4.69E-02	-1.97E-06	-2.46E-05	1.15E-06
-3.34E-02	-1.41E-06	-1.77E-05	5.90E-07
-2.01E-02	-8.36E-07	-1.05E-05	2.10E-07
-6.67E-03	-3.02E-07	-3.77E-06	2.51E-08
6.70E-03	2.54E-07	3.17E-06	2.13E-08
2.01E-02	8.27E-07	1.03E-05	2.08E-07
3.36E-02	1.36E-06	1.70E-05	5.72E-07
4.70E-02	1.93E-06	2.41E-05	1.13E-06
6.04E-02	2.49E-06	3.11E-05	1.88E-06
7.38E-02	3.06E-06	3.82E-05	2.82E-06
8.72E-02	3.66E-06	4.57E-05	3.98E-06
1.01E-01	4.21E-06	5.26E-05	5.30E-06
1.14E-01	4.81E-06	6.02E-05	6.86E-06
1.27E-01	5.43E-06	6.79E-05	8.66E-06

1.41E-01	6.05E-06	7.56E-05	1.07E-05
1.54E-01	6.70E-06	8.38E-05	1.29E-05
1.68E-01	7.38E-06	9.22E-05	1.55E-05
1.81E-01	8.03E-06	1.00E-04	1.82E-05
1.95E-01	8.75E-06	1.09E-04	2.13E-05
2.08E-01	9.43E-06	1.18E-04	2.45E-05
2.22E-01	1.02E-05	1.28E-04	2.82E-05
2.35E-01	1.09E-05	1.36E-04	3.20E-05
2.48E-01	1.18E-05	1.47E-04	3.66E-05
2.62E-01	1.27E-05	1.59E-04	4.17E-05
2.75E-01	1.38E-05	1.72E-04	4.73E-05
2.89E-01	1.48E-05	1.86E-04	5.36E-05
3.02E-01	1.61E-05	2.02E-04	6.09E-05
3.15E-01	1.76E-05	2.20E-04	6.94E-05
3.29E-01	1.93E-05	2.41E-04	7.94E-05
3.42E-01	2.13E-05	2.66E-04	9.11E-05
3.56E-01	2.37E-05	2.96E-04	1.05E-04
3.69E-01	2.66E-05	3.32E-04	1.23E-04
3.83E-01	3.01E-05	3.76E-04	1.44E-04
3.96E-01	3.43E-05	4.29E-04	1.70E-04
4.09E-01	3.94E-05	4.93E-04	2.02E-04
4.23E-01	4.54E-05	5.67E-04	2.40E-04
4.36E-01	5.25E-05	6.57E-04	2.86E-04
4.50E-01	6.07E-05	7.59E-04	3.41E-04
4.63E-01	7.03E-05	8.78E-04	4.07E-04
4.77E-01	8.11E-05	1.01E-03	4.83E-04
4.90E-01	9.34E-05	1.17E-03	5.72E-04
5.03E-01	1.07E-04	1.34E-03	6.73E-04
5.17E-01	1.23E-04	1.53E-03	7.92E-04
5.30E-01	1.40E-04	1.75E-03	9.26E-04
5.44E-01	1.58E-04	1.98E-03	1.08E-03
5.57E-01	1.79E-04	2.24E-03	1.25E-03
5.70E-01	2.01E-04	2.51E-03	1.43E-03
5.84E-01	2.25E-04	2.81E-03	1.64E-03
5.97E-01	2.50E-04	3.12E-03	1.86E-03
6.11E-01	2.77E-04	3.46E-03	2.11E-03
6.24E-01	3.05E-04	3.81E-03	2.38E-03
6.38E-01	3.35E-04	4.19E-03	2.67E-03
6.51E-01	3.66E-04	4.58E-03	2.98E-03
6.64E-01	3.99E-04	4.99E-03	3.32E-03
6.78E-01	4.33E-04	5.42E-03	3.67E-03
6.91E-01	4.69E-04	5.86E-03	4.05E-03
7.05E-01	5.06E-04	6.32E-03	4.45E-03
7.18E-01	5.44E-04	6.80E-03	4.88E-03
7.32E-01	5.83E-04	7.29E-03	5.33E-03
7.45E-01	6.24E-04	7.79E-03	5.81E-03
7.58E-01	6.66E-04	8.32E-03	6.31E-03
7.72E-01	7.09E-04	8.86E-03	6.84E-03
7.85E-01	7.53E-04	9.41E-03	7.39E-03
7.99E-01	7.99E-04	9.98E-03	7.97E-03
8.12E-01	8.45E-04	1.06E-02	8.58E-03
8.26E-01	8.93E-04	1.12E-02	9.22E-03
8.39E-01	9.42E-04	1.18E-02	9.88E-03
8.52E-01	9.92E-04	1.24E-02	1.06E-02
8.66E-01	1.04E-03	1.30E-02	1.13E-02
8.79E-01	1.10E-03	1.37E-02	1.20E-02
8.93E-01	1.15E-03	1.44E-02	1.28E-02
9.06E-01	1.20E-03	1.51E-02	1.36E-02

9.19E-01	1.26E-03	1.57E-02	1.45E-02
9.33E-01	1.32E-03	1.65E-02	1.54E-02
9.46E-01	1.37E-03	1.72E-02	1.63E-02
9.60E-01	1.43E-03	1.79E-02	1.72E-02
9.73E-01	1.49E-03	1.87E-02	1.82E-02
9.87E-01	1.56E-03	1.94E-02	1.92E-02
1.00E+00	1.62E-03	2.02E-02	2.02E-02

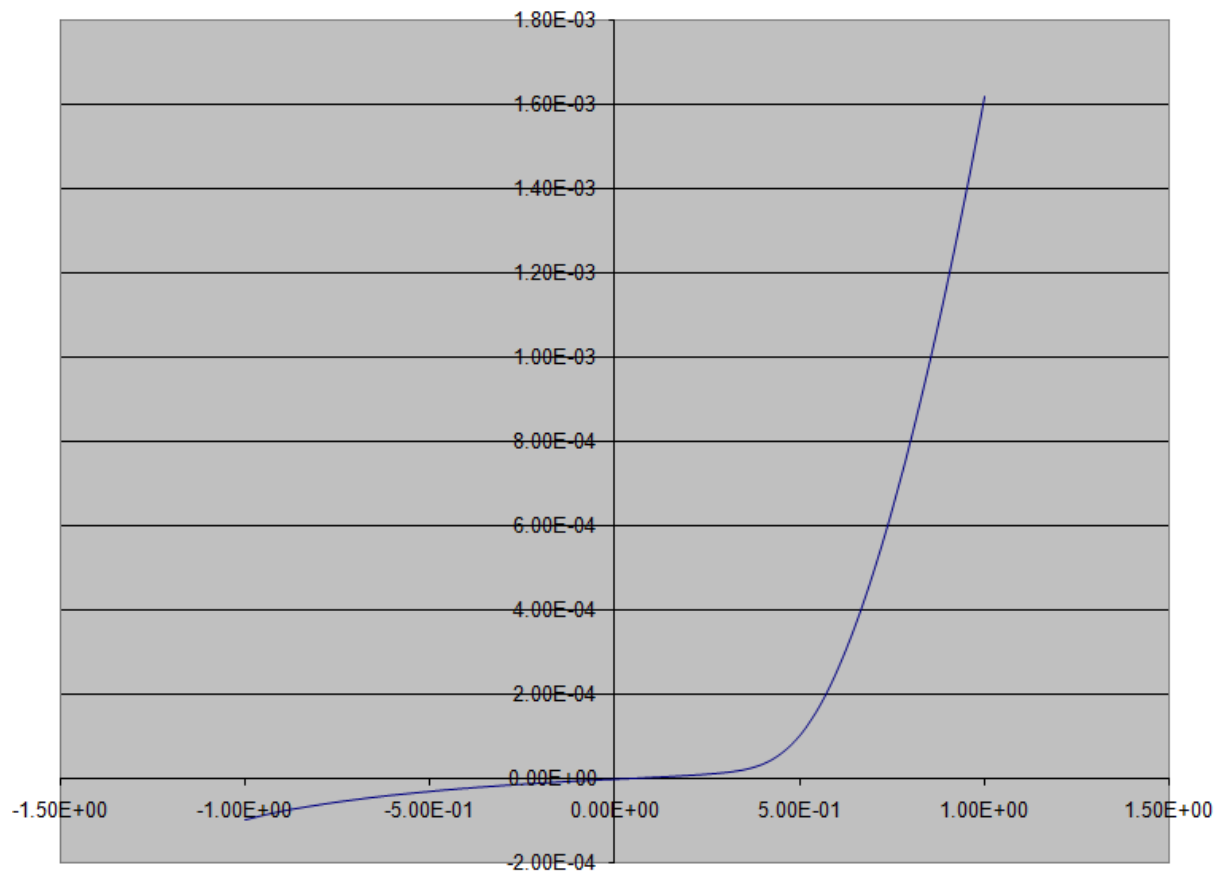


Fig 6.26 Cell characteristics in dark

6.5.1 CALCULATIONS

From the characterization data obtained in light we get:

$$I_{SC} = 5.46 \times 10^{-4}$$

$$V_{OC} = 4.76 \times 10^{-1}$$

$$\text{Cell Area} = 8.1 \text{ mm}^2$$

$$J_{SC} = (I_{SC}/\text{Area}) = 6.74 \times 10^{-3}$$

$$\text{Fill Factor} = [(J_{SC \text{ (MAX)}} \times V_{MAX}) / (J_{SC} \times V_{OC})]$$

$$J_{SC \text{ (MAX)}} = 2.62 \times 10^{-1}, V_{MAX} = 4.51 \times 10^{-3}$$

$$\text{Therefore, Fill Factor} = 0.3683$$

$$\text{Power Input} = 100 \text{ mW/cm}^2$$

$$\text{Efficiency } (\eta) = [(P_{MAX} / 100) \times 1000 \times 100] \text{ where } P_{MAX} = J_{SC \text{ (MAX)}} \times V_{MAX}$$

$$P_{MAX} = 11.81 \times 10^{-2}$$

$$\text{Therefore, Efficiency } (\eta) == \mathbf{1.18\%}$$